ELSEVIER

As-quenched microstructures of $Cu_{3-x}Mn_xAl$ alloys

S.Y. Yang, T.F. Liu *

Department of Materials Science and Engineering, National Chiao Tung University, Taiwan, ROC

Received 21 June 2005; accepted 21 September 2005

Abstract

In the as-quenched condition, the microstructure of the $Cu_{2.9}Mn_{0.1}Al$ alloy was of $D0_3$ phase containing γ'_1 martensite. This is similar to that reported by other workers in the Cu_3Al alloy. However, the as-quenched microstructure of the $Cu_{2.8}Mn_{0.2}Al$ or $Cu_{2.7}Mn_{0.3}Al$ alloy were found to be of $D0_3$ phase containing extremely fine L-J precipitates, whereas for $Cu_{2.6}Mn_{0.4}Al$ alloy, it was a mixture of $(D0_3 + L2_1 + L-J)$ phases. These results are different from those proposed by Bouchard et al.
© 2005 Elsevier B.V. All rights reserved.

Keywords: $Cu_{3-x}Mn_xAl$ alloy; γ'_1 Martensite; L-J phase; $a/4\langle 1\,1\,1\rangle$ anti-phase boundary

1. Introduction

By using thermal analysis method, Bouchard et al. have established the $Cu_{3-x}Mn_xAl$ ($0 \leqq X \leqq 1$) metastable phase diagram [1]. In that phase diagram, it is seen that when the $Cu_{3-x}Mn_xAl$ alloys with $0.1 \leqq X \leqq 0.8$ were solution-treated in the single β-phase (disordered body-centered cubic (bcc)) region followed by a rapid quench into iced brine, a $\beta \rightarrow B2 \rightarrow D0_3 + L2_1$ transition would occur by an ordering transition and a spinodal decomposition process, respectively. When the manganese (Mn) content in the $Cu_{3-x}Mn_xAl$ alloys was increased to 25 at.% ($X = 1$), the as-quenched microstructure of the Cu_2MnAl alloy became a single $L2_1$ phase. In addition to the thermal analysis method, transmission electron microscopy (TEM) was also used by many workers to examine the as-quenched microstructures of the $Cu_{3-x}Mn_xAl$ alloys with $0.5 \leqq X \leqq 1.0$ [1–4]. These results were found to be consistent with those proposed by Bouchard et al.

Recently, we made TEM observations on the phase transformations of a $Cu_{2.2}Mn_{0.8}Al$ alloy [5]. Our experimental result indicated that the as-quenched microstructure of the $Cu_{2.2}Mn_{0.8}Al$ alloy consisted of a mixture of $(D0_3 + L2_1 + L-J)$ phases, where the L-J phase is a new phase having an orthorhombic structure with lattice parameters $a = 0.413$ nm, $b = 0.254$ nm and $c = 0.728$ nm [5]. This result is quite different from that reported by previous workers. However, to date, all of the TEM examinations were focused on the $Cu_{3-x}Mn_xAl$ alloys with $0.5 \leqq X \leqq 1$. Little information concerning the $Cu_{3-x}Mn_xAl$ alloys with lower Mn content has been provided. Therefore, the purpose of the present study is to investigate the as-quenched microstructures of the $Cu_{3-x}Mn_xAl$ alloys with $X < 0.5$.

2. Experimental procedure

Four alloys, $Cu_{2.9}Mn_{0.1}Al$ (Cu–2.5 at.% Mn–25.0 at.% Al), $Cu_{2.8}Mn_{0.2}Al$ (Cu–5.0 at.% Mn–25.0 at.% Al), $Cu_{2.7}Mn_{0.3}Al$ (Cu–7.5 at.% Mn–25.0 at.% Al) and $Cu_{2.6}Mn_{0.4}Al$ (Cu–10.0 at.% Mn–25.0 at.% Al), were prepared in a vacuum induction furnace under a controlled protective Ar atmosphere by using 99.99% Cu, 99.9% Mn and 99.99% Al. The melts were chill cast into $30\,mm \times 50\,mm \times 200\,mm$ copper molds. After being homogenized at 900 °C for 72 h, the ingots were sectioned into 2-mm thick slices. These slices were subsequently solution-treated at 850 °C for 1 h (in the single β-phase state) followed by a rapid quench into iced brine.

TEM specimens were prepared by means of a double-jet electropolisher with an electrolyte of 70% methanol and 30% nitric acid. The polishing temperature was kept in the range from −30 to −15 °C, and the current density was kept in the range from 3.0×10^4 to 4.0×10^4 A m^{-2}. Electron microscopy was performed on a JEOL JEM-2000FX scanning transmission electron microscope operating at 200 KV.

3. Results and discussion

Fig. 1(a) is a bright-field (BF) electron micrograph of the as-quenched $Cu_{2.9}Mn_{0.1}Al$ alloy, clearly exhibiting a second phase with a plate-like morphology within the matrix. Fig. 1(b) and (c) show two selected-area diffraction patterns (SADPs) taken from a plate-like phase and its surrounding matrix. In these SADPs, it is seen that beside those reflection spots corresponding to the

* Corresponding author. Tel.: +886 3 5731675; fax: +886 3 5728504.
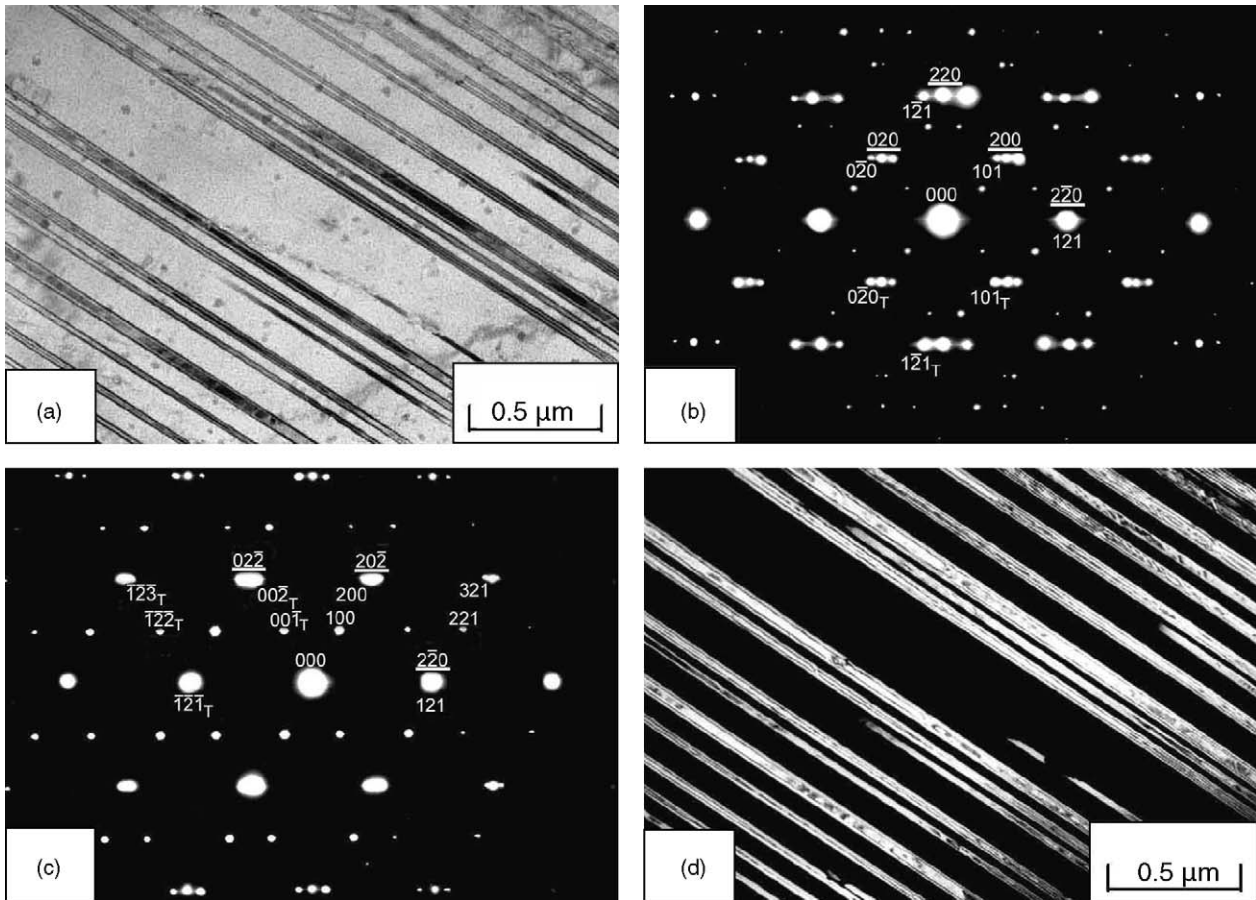 *E-mail address:* tfliu@cc.nctu.edu.tw (T.F. Liu).

Fig. 1. Electron micrographs of the as-quenched $Cu_{2.9}Mn_{0.1}Al$ alloy. (a) BF, (b) and (c) two SADPs. The zone axes of the D0$_3$ phase, γ'_1 martensite and internal twin are (b) [0 0 1], [1 0 $\bar{1}$] and [$\bar{1}$ 0 1]; (c) [1 1 1], [0 1 $\bar{2}$] and [$\bar{2}$ 1 0], respectively ($\underline{hkl}$ = D0$_3$ phase, hkl = γ'_1 martensite, hkl_T = internal twin). (d) (1 $\bar{2}$ 1) γ'_1 DF.

D0$_3$ phase [6–9], extra spots caused by the second phase are clearly visible. Compared with the previous studies in Cu–Al and Cu–Al–Ni alloys [9–11], it can be realized that the positions and streaking behaviors of the extra spots are the same as those of the γ'_1 martensite with internal twins. The γ'_1 martensite has an orthorhombic structure with lattice parameters $a = 0.440$ nm, $b = 0.534$ nm and $c = 0.422$ nm [9,12]. Fig. 1(d) is a (1 $\bar{2}$ 1) γ'_1 dark-field (DF) electron micrograph, clearly revealing the presence of the plate-like γ'_1 martensite. Accordingly, it is concluded that the as-quenched microstructure of the $Cu_{2.9}Mn_{0.1}Al$ alloy was D0$_3$ phase containing plate-like γ'_1 martensite. This finding is similar to that reported by other workers in the Cu$_3$Al alloy [1,10].

When the Mn content was increased to 5.0 at.%, no evidence of the γ'_1 martensite could be detected, rather a high density of extremely fine precipitates with a mottled structure could be observed within the D0$_3$ matrix. A typical example is shown in Fig. 2. Fig. 2(a) is a BF electron micrograph of the $Cu_{2.8}Mn_{0.2}Al$ alloy in the as-quenched condition. Fig. 2(b) and (c) show two SADPs of the as-quenched alloy. When compared with our previous studies in the $Cu_{2.2}Mn_{0.8}Al$ and Cu–14.2Al–7.8Ni alloys [5,9], it is found, in these SADPs, that the extra spots with streaks could be derived from the L-J phase with two variants. Fig. 2(d) is a ($\bar{1}$ 1 1) D0$_3$ DF electron micrograph of the same area as Fig. 2(a), revealing the presence of the fine D0$_3$ domains with

$a/2\langle 1\,0\,0\rangle$ anti-phase boundaries (APBs). Fig. 2(e), a (0 0 2) D0$_3$ DF electron micrograph, shows the presence of the small B2 domains with $a/4\langle 1\,1\,1\rangle$ APBs. In Fig. 2(d) and (e), it is seen that the sizes of both D0$_3$ and B2 domains are very small. Therefore, it is deduced that the D0$_3$ phase present in the as-quenched alloy was formed by a $\beta \rightarrow$ B2 $\rightarrow$ D0$_3$ continuous ordering transition during quenching [13–15]. Fig. 2(f) is a (1 0 0$_1$) L-J DF electron micrograph, exhibiting the presence of the extremely fine L-J precipitates. Based on the above observations, it was concluded that the as-quenched microstructure of the $Cu_{2.8}Mn_{0.2}Al$ alloy was D0$_3$ phase containing extremely fine L-J precipitates, where the D0$_3$ phase was formed by the $\beta \rightarrow$ B2 $\rightarrow$ D0$_3$ continuous ordering transition during quenching.

Transmission electron microscopy examinations of thin foils indicated that the as-quenched microstructure of the $Cu_{2.7}Mn_{0.3}Al$ alloy was also D0$_3$ phase containing extremely fine L-J precipitates, which is similar to that observed in the $Cu_{2.8}Mn_{0.2}Al$ alloy. An example is shown in Fig. 3. By comparing Figs. 2 and 3, it is clear that a slight increase of the Mn content would significantly raise the amount of the L-J precipitates, it would also increase the sizes of both B2 and D0$_3$ domains.

Fig. 4(a) is a BF electron micrograph of the as-quenched $Cu_{2.6}Mn_{0.4}Al$ alloy, exhibiting a modulated structure. Shown in Fig. 4(b) is an SADP of the as-quenched alloy. In this figure, it is seen that in addition to the reflection spots with streaks
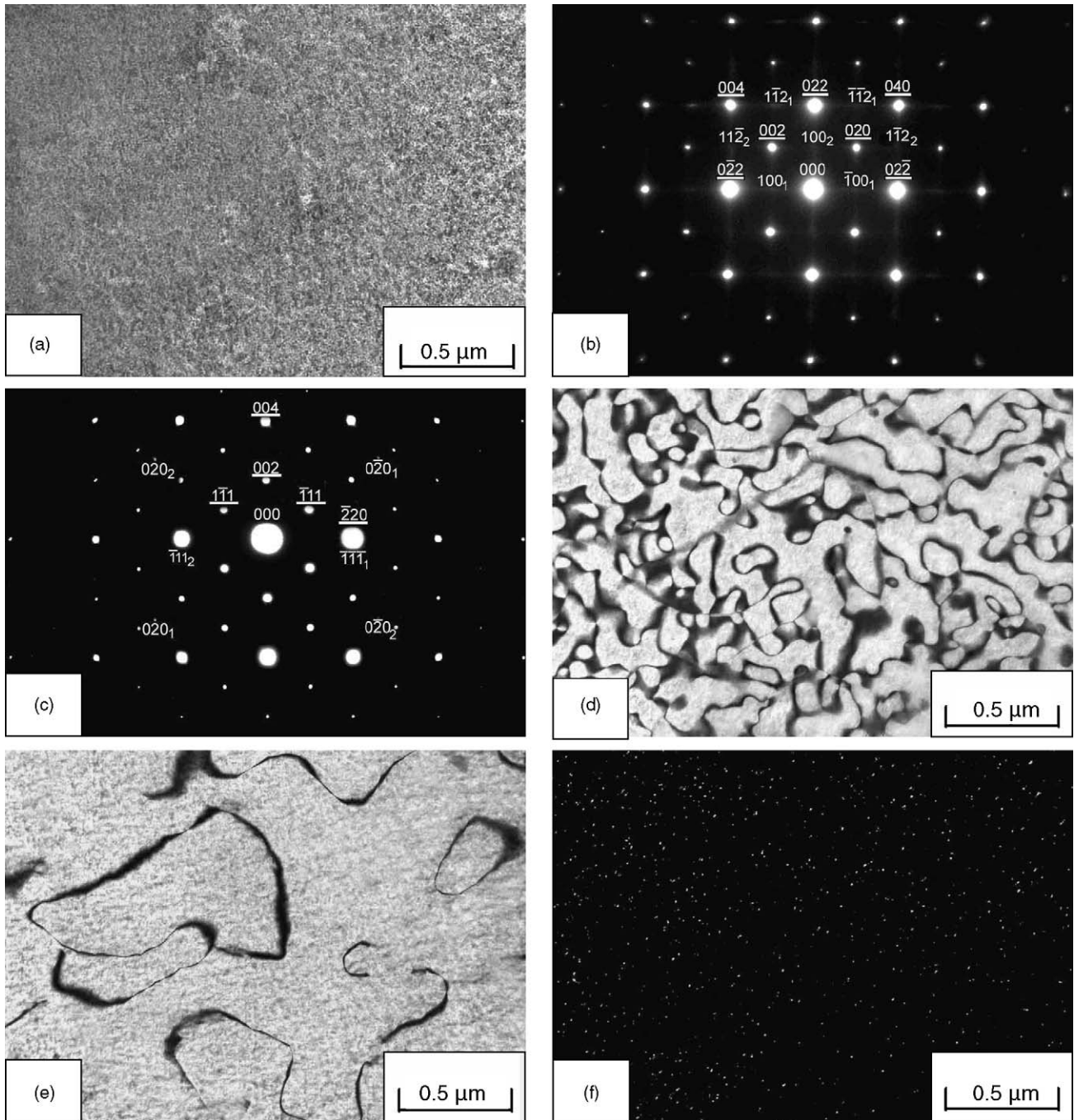
Fig. 2. Electron micrographs of the as-quenched $Cu_{2.8}Mn_{0.2}Al$ alloy. (a) BF, (b) and (c) two SADPs. The zone axes of the $D0_3$ phase are (b) [1 0 0] and (c) [1 1 0], respectively, ($\underline{hkl} = D0_3$ phase, $hkl_{1 or 2} = $ L-J phase; 1: variant 1, 2: variant 2). (d) and (e) $(\bar{1} 1 1)_{D0_3}$ and $(0 0 2)_{D0_3}$ DF, respectively, (f) $(1 0 0_1)_{L-J}$ DF.

of the L-J phase, the superlattice reflection spots with satellites lying along $\langle 0 0 1 \rangle$ reciprocal lattice directions could be clearly observed. Compared with the previous studies in the $Cu_{3-x}Mn_xAl$ alloys with $x = 0.5$ or $x = 0.8$ [1,5], it is obvious that these supperlattice reflection spots with satellites were attributed to the coexistence of the $(D0_3 + L2_1)$ phases. The $(D0_3 + L2_1)$ phases could be formed via the $\beta \rightarrow B2 \rightarrow D0_3 + L2_1$ transition during quenching. Fig. 4(c), a $(\bar{1} 1 1)$ $D0_3$ DF electron micrograph, reveals the presence of the $D0_3$ domains with $a/2\langle 1 0 0 \rangle$ APBs. Fig. 4(d) is a $(0 0 2)$ $D0_3$ DF electron micrograph; no

evidence of the $a/4\langle 1 1 1 \rangle$ APBs could be detected. This feature is similar to that observed in the as-quenched $Cu_{3-x}Mn_xAl$ alloys with $0.5 \leqq X \leqq 1.0$ [1,2,5]. Fig. 4(e), a DF electron micrograph taken with the $(1 0 0_1)$ L-J reflection spot, exhibits that the amount of the extremely fine L-J precipitates was greater than that observed in Figs. 2 and 3. As a consequence, the as-quenched microstructure of the $Cu_{2.6}Mn_{0.4}Al$ alloy was the mixture of $(D0_3 + L2_1 + L-J)$ phases.

On the basis of the preceding results, it can be concluded that in the as-quenched condition, the L-J phase was present

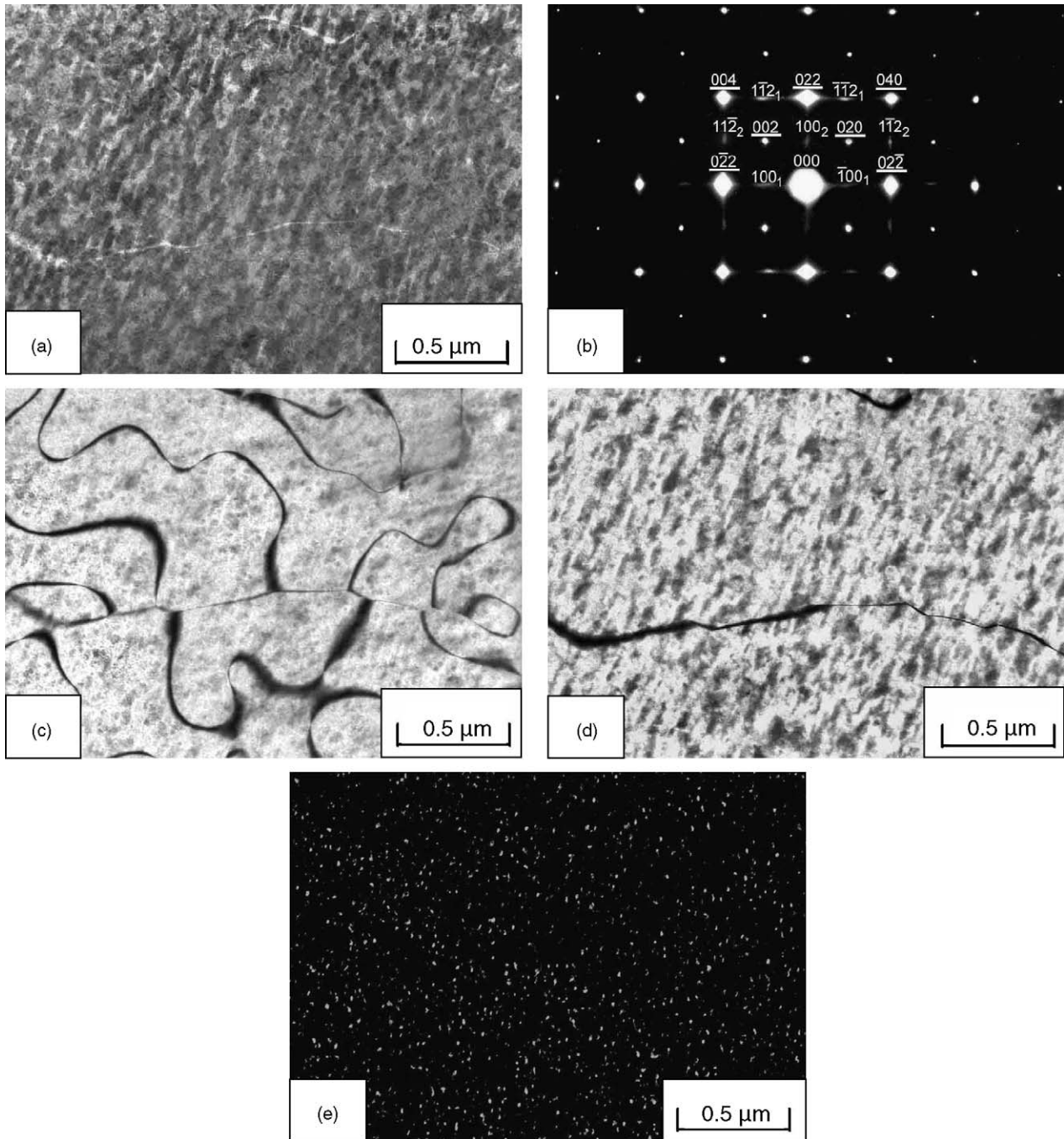Fig. 3. Electron micrographs of the as-quenched $Cu_{2.7}Mn_{0.3}Al$ alloy. (a) BF, (b) an SADP. The zone axis of the $D0_3$ phase is $[1\,0\,0]$ ($\underline{hkl} = D0_3$ phase, $hkl_{1or2} = $L-J phase; 1: variant 1, 2: variant 2). (c) and (d) $(\bar{1}\,1\,1)_{D0_3}$ and $(0\,0\,2)_{D0_3}$ DF, respectively. (e) $(1\,0\,0_1)_{L-J}$ DF.

in the $Cu_{3-x}Mn_xAl$ alloys with $X = 0.2$, 0.3 and 0.4, whose amount increased with increasing Mn content. Besides, the $\beta \rightarrow B2 \rightarrow D0_3 + L2_1$ transition had occurred during quenching in the $Cu_{2.6}Mn_{0.4}Al$ alloy. These observations are consistent with those proposed by Bouchard et al. [1]. However, when the $Cu_{3-x}Mn_xAl$ alloys with $X = 0.1$, 0.2 and 0.3 were solution-treated followed by a rapid quench, the $\beta \rightarrow B2 \rightarrow D0_3$ transition instead of the $\beta \rightarrow B2 \rightarrow D0_3 + L2_1$ transition was found to occur. This finding is different from the previous proposition in the $Cu_{3-x}Mn_xAl$ alloys with $0.1 \leqq X \leqq 0.8$ [1].

In Fe–Al and Fe–Al–Mn alloys, it is well-known that if the $D0_3$ phase was formed by continuous ordering transition during quenching, it would always occur through an A2 (disordered body-centered cubic) $\rightarrow B2 \rightarrow D0_3$ transition. The A2 $\rightarrow$ B2 transition produced the $a/4\langle 1\,1\,1 \rangle$ APBs and the B2 $\rightarrow D0_3$ transition produced the $a/2\langle 1\,0\,0 \rangle$ APBs [13–15]. However, to date, no $a/4\langle 1\,1\,1 \rangle$ APBs could be investigated by other workers in the as-quenched $Cu_{3-x}Mn_xAl$ alloys [1–2,5]. In the present study, it is obvious that no evidence of the $a/4\langle 1\,1\,1 \rangle$ APBs could be observed in the $Cu_{2.6}Mn_{0.4}Al$ alloy. However, when the Mn
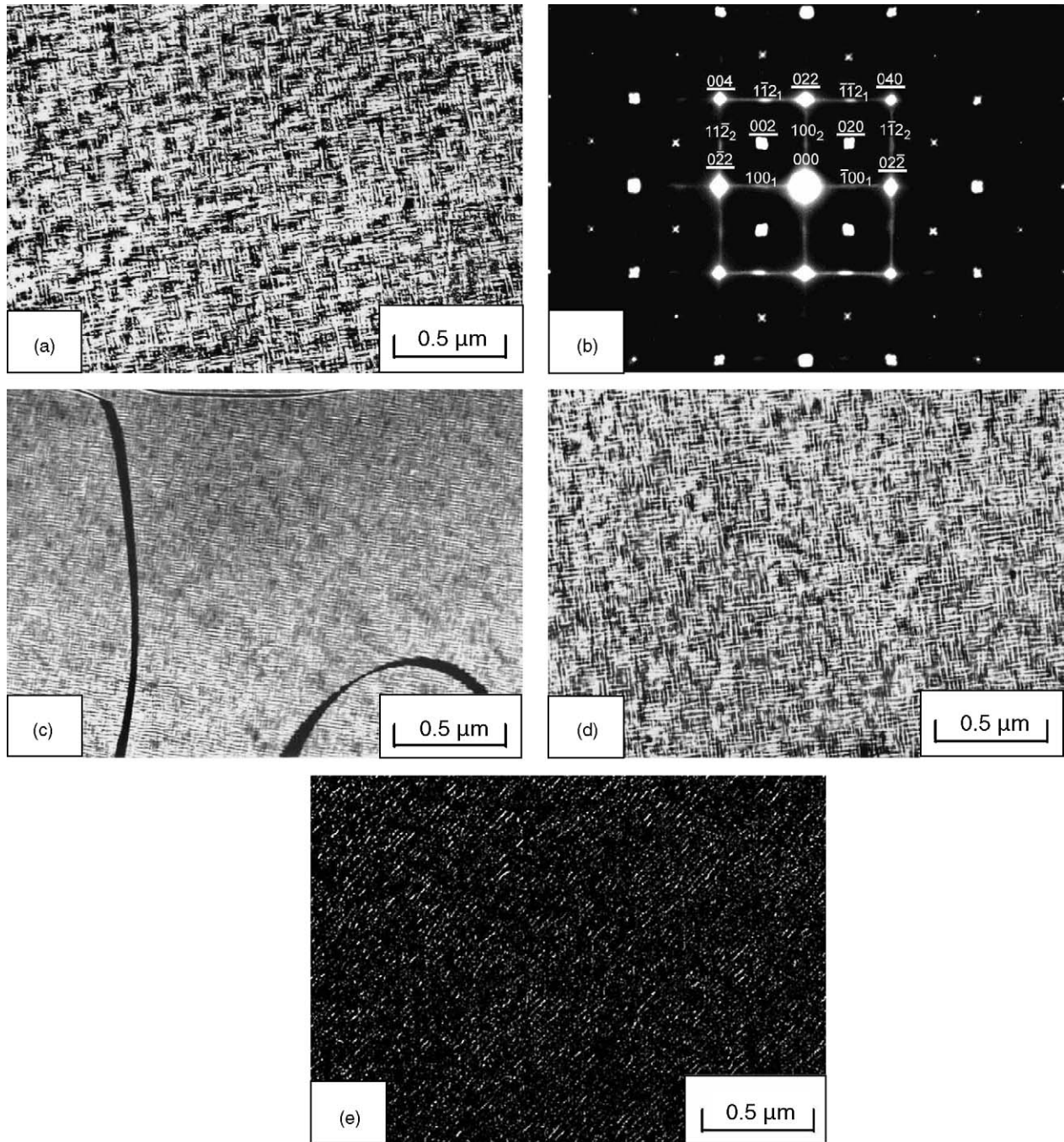
Fig. 4. Electron micrographs of the as-quenched $Cu_{2.6}Mn_{0.4}Al$ alloy. (a) BF, (b) an SADP. The zone axis of the $D0_3$ phase is [1 0 0]. ($\underline{hkl} = D0_3 + L2_1$ phase, $hkl_{1or2} = $ L-J phase; 1: variant 1, 2: variant 2). (c) and (d) $(\bar{1} 1 1)_{D0_3}$ and $(0 0 2)_{D0_3}$ DF, respectively, (e) $(1 0 0_1)_{L-J}$ DF.

content was decreased to 7.5 at.% or below, the $a/4\langle 1 1 1\rangle$ APBs became visible, as shown in Figs. 2(e) and 3(d). This result implies that in the $Cu_{3-x}Mn_xAl$ alloys, an increase of the Mn content would increase the B2 domain size significantly. When the Mn content increased to above 10.0 at.%, the B2 domain size would consume to the whole grain during quenching. Therefore, no $a/4\langle 1 1 1\rangle$ APBs could be detected. This may be one possible reason to account for the absence of the $a/4\langle 111\rangle$ APBs in the previous studies of the as-quenched $Cu_{3-x}Mn_xAl$ alloys with $0.5 \leqq X \leqq 1.0$ [1,2,5].

Finally, it is worthwhile to note that the size of the $D0_3$ domains increased with increasing the Mn content. This implies that an increase of the Mn content would increase the B2 → $D0_3$ ordering transition temperature. This result is comparable to that obtained by Bouchard et al. [1].

4. Conclusions

1. The as-quenched microstructure of the $Cu_{2.9}Mn_{0.1}Al$ alloy was of $D0_3$ phase containing plate-like γ'_1 martensite. This

is similar to that reported by other workers in the Cu_3Al alloy.

2. The as-quenched microstructure of the $Cu_{2.8}Mn_{0.2}Al$ or $Cu_{2.7}Mn_{0.3}Al$ alloy was of $D0_3$ phase containing extremely fine L-J precipitates, where the $D0_3$ phase was formed through the $\beta \rightarrow B2 \rightarrow D0_3$ transition during quenching.

3. The as-quenched microstructure of the $Cu_{2.6}Mn_{0.4}Al$ alloy was a mixture of $(D0_3 + L2_1 + \text{L-J})$ phases, where the $(D0_3 + L2_1)$ phases were formed through the $\beta \rightarrow B2 \rightarrow D0_3 + L2_1$ transition during quenching.

4. The sizes of both B2 and $D0_3$ domains increased with increasing Mn content. In the $Cu_{2.8}Mn_{0.2}Al$ and $Cu_{2.7}Mn_{0.3}Al$ alloys, the $a/4\langle 1\,1\,1 \rangle$ APBs could be clearly observed. However, no evidence of the $a/4\langle 1\,1\,1 \rangle$ APBs could be detected in the $Cu_{2.6}Mn_{0.4}Al$ alloy.

5. The amount of the L-J precipitates increased with increasing the Mn content.

Acknowledgments

References

[1] M. Bouchard, G. Thomas, Acta Metall. 23 (1975) 1485.
[2] Y.G. Nesterenko, I.A. Osipenko, S.A. Firstov, Fiz. Met. Metalloved. 27 (1969) 135.
[3] Y.G. Nesterenko, I.A. Osipenko, Fiz. Met. Metalloved. 36 (1973) 702.
[4] R. Kozubski, J. Soltys, J. Dutkiewicz, J. Morgiel, J. Mater. Sci. 22 (1987) 3843.
[5] S.C. Jeng, T.F. Liu, Metall. Mater. Trans. A 26A (1995) 1353.
[6] T.F. Liu, J.S. Chou, C.C. Wu, Metall. Trans. A 21A (1991) 1891.
[7] T.F. Liu, G.C. Uen, C.Y. Chao, Y.L. Lin, C.C. Wu, Metall. Trans. A 22A (1991) 1407.
[8] C.C. Wu, J.S. Chou, T.F. Liu, Metall. Trans. A. 22A (1991) 2265.
[9] C.H. Chen, T.F. Liu, Metall. Mater. Trans. A 34A (2003) 503.
[10] F.C. Lovey, V.G. Tendeloo, V.J. Landuyt, S. Amelinckx, Scripta Metall. 19 (1985) 1223.
[11] N. Kuwano, C.M. Wayman, Metall. Trans. A 15A (1984) 621.
[12] T. Hara, T. Ohba, S. Miyazaki, K. Otsuka, Mater. Trans. JIM 33 (1992) 1105.
[13] P.R. Swann, W.R. Duff, R.M. Fisher, Metall. Trans. 3 (1972) 409.
[14] S.M. Allen, J.W. Chan, Acta Metall. 24 (1976) 425.
[15] J.W. Lee, T.F. Liu, Mater. Chem. Phys. 69 (2001) 192.